Journal of Applied Electrochemistry **33**: 1137–1142, 2003.

A nonlinear kinetic model introduced for the corrosion inhibitive properties of some organic inhibitors

S. MARTINEZ and M. METIKOŠ-HUKOVIĆ*
Department of Electrochemistry, Faculty of Chemical Engineering and Technology, University of Zagreb, Savska c.16, P.O. Box 177, HR-10000 Zagreb, Croatia
*(*author for correspondence, e-mail: mmetik@marie.fkit.hr)*

Received 21 March 2003; accepted in revised form 18 July 2003

Key words: acid corrosion, adsorption, corrosion inhibitor, low-carbon steel, tannin

Abstract

Corrosion kinetics of low-carbon steel in hydrochloric acid was studied at various concentrations of mimosa tannin inhibitor. This system was subjected to impedance spectroscopy and quasi steady-state polarization. The inhibition efficiency, η was derived from the corrosion current, i_{corr} and charge transfer resistance, R_{ct} data. The fractional surface coverage as a function of the inhibitor concentration was calculated from the rate of hydrogen evolution reaction (h.e.r.) at constant cathodic potential. Based on the theoretical model and the observed experimental relationship between the ratio of the corrosion current densities in the uninhibited and the inhibited systems and the surface coverage, the relative influences of the geometric blocking action and the energy effect of the inhibitor on the corrosion process were estimated. Fitting of the nonlinear model to the experimental data was carried out by the Levnberg–Marquardt nonlinear fit method implemented into the programming system *Mathematica*®. Restructuring of the adsorbed layer and change in the orientation of adsorbed inhibitor molecules upon the increase of surface coverage was assumed on the basis of the experimentally observed functional relationship of the double layer capacitance and the surface coverage. The results were explained with respect to the molecular properties of the inhibitor – geometry and size of the molecule, electronic orbital structure and dipole moment.

List of symbols

b_a	anodic Tafel slope (V dec^{-1})
b_c	cathodic Tafel slope (V dec^{-1})
b_0	constant equal to RT/F (V)
C_{dl}	double layer capacity (F m^{-2})
C_1	specific capacity in the base electrolyte (F m^{-2})
C_2	specific capacity of the surface covered by the flat-lying molecules (F m^{-2})
C_3	specific capacity of the surface covered by the perpendicular molecules (F m^{-2})
c_{inh}	inhibitor concentration (mol m^{-3})
E_{ocp}	open circuit potential (V)
E_{SCE}	electrode potential vs. saturated calomel electrode (V)
I	imaginary constant
i_a	partial anodic current density in the uninhibited system (A m^{-2})
i'_a	partial anodic current density in the inhibited system (A m^{-2})
i_c	partial cathodic current density in the uninhibited system (A m^{-2})
i'_c	partial cathodic current density in the inhibited system (A m^{-2})
i_{cat}	cathodic current density (A m^{-2})
i_{corr}	corrosion current density in the uninnhibited system (A m^{-2})
i'_{corr}	corrosion current density in the inhibited system (A m^{-2})
k	constant
k_1	cathodic reaction rate constant (A m^{-2})
k_2	anodic reaction rate constant (A m^{-2})
m	dimensionless model parameter
N	Avogadro's constant (mol^{-1})
n	dimensionless model parameter
Q	capacitance model parameter (Ω^{-1} s^n m^{-2})
R	universal gas constant (J mol^{-1} K^{-1})
R_{ct}	charge transfer resistance (Ω m^2)
R_s	solution resistance (Ω m^2)
T	temperature (K)
Z_{total}	impedance of the equivalent circuit (Ω m^2)
γ	ratio of the corrosion currents in the noninhibited and inhibited systems
γ_{imp}	γ from impedance measurements
γ_{pol}	γ from polarization measurements
η_{imp}	inhibitor efficiency from impedance measurements (%)
η_{pol}	inhibitor efficiency from polarization measurements (%)
α	transfer coefficient of the cathodic reaction

β transfer coefficient of the anodic reaction
ϕ potential (V)
ϕ_{corr} corrosion potential in the uninhibited system (V)
ϕ'_{corr} corrosion potential in the inhibited system (V)
θ surface coverage
ψ_1 potential drop in the diffusion part of the double layer (V)
$\Delta\psi_1$ change of the potential drop in the diffusion part of the double layer (V)
ψ_1^0 ψ_1 of the uninhibited system (V)

1. Introduction

The proposed mechanism of most organic inhibitors in aggressive acid media is adsorption [1–5]. The adsorption process depends on the electronic characteristics of the inhibitor, the nature of the surface, the temperature and pH of the corrosion media, steric effects, multilayer adsorption and a varying degree of surface-site activity [6–8]. In principle, adsorption of an organic inhibitor can affect the corrosion rate in two ways: by decreasing the available reaction area (geometric blocking effect) and by modifying the activation energy of the anodic and/or cathodic reactions occurring on the inhibitor-free surface in the course of the inhibited corrosion process. The electrochemical behaviour and the interpretation of the measured data will not be the same for all modes.

In acidic solutions, in the presence of an adsorbed substance on the electrode surface, the following expressions are valid for the cathodic evolution of hydrogen and anodic dissolution of metals [9, 10]:

$$i'_c = k_1[H_3O^+](1-\theta)e^{-\frac{F}{RT}[\alpha\phi+(1-\alpha)\psi_1]} \quad (1a)$$

$$i'_a = k_2(1-\theta)e^{\frac{F}{RT}2\beta(\phi-\psi_1)} \quad (1b)$$

where ψ_1 is the potential drop in the diffuse part of the double layer. All the factors that influence the potential ψ_1 will likewise alter the corrosion rate. The surface blocking effect expressed through the factor $(1-\theta)$ and the energy effect expressed through the change in $\psi_1 = \psi_1^0 + \Delta\psi_1$ may act in the same or opposite directions. For example, the adsorption of substances of cationic type or neutral polar molecules with the positive side of their dipoles oriented towards the electrode will induce a positive change in ψ_1 or $\Delta\psi_1 > 0$ and consequently impede the corrosion reactions. On the other hand, adsorption of anions and/or neutral polar molecules with the negative side of their dipoles oriented towards the electrode will induce a negative change in ψ_1 or $\Delta\psi_1 < 0$ and the overall retarding or accelerating effect on the rate of corrosion reactions will depend on the relative influences of θ and ψ_1, respectively. Additionally, stimulation of corrosion in the presence of adsorbed organic substances may be caused by factors other than the shift in ψ_1, for example: the formation of soluble complexes by metal ions with the adsorbed substance lowering the overpotential of the anodic reaction, or the reduction of organic substance, or the catalytic action of the adsorbed substance on hydrogen evolution lowering the overpotential of the cathodic reaction.

In the limit of $\Delta\psi_1 \to 0$ and $\theta \to 0$, the Equations (1a) and (1b) reduce to those valid for the inhibitor-free system. By making use of the equality of the anodic and cathodic currents at the corrosion potential, both in the inhibited and the uninhibited systems, the following variation in the steady-state potential may be derived [10]:

$$\phi_{corr} - \phi'_{corr} = \Delta\psi_1\left[\frac{b_a b_c}{b_0(b_a+b_c)} - 1\right] \quad (2)$$

where b_a and b_c are the anodic and the cathodic Tafel slopes in the inhibitor-free solution, and $b_0 = RT/F$. For the case of the geometric blocking action, $\Delta\psi_1 = 0$, and, theoretically, no shift in the corrosion potential will be observed upon addition of the inhibitor to the system.

It is apparent from the above considerations that it is difficult in each specific case to calculate which part of the inhibiting effect is connected to the geometric blocking action and which part is connected to the energy effect. A comparison of either of the two current components, anodic or cathodic, in the uninhibited and inhibited systems at the corresponding corrosion potentials, with the assumption that ψ_1 changes linearly with θ (i.e. $\psi_1 = \psi_1^0 + k\theta$), the ratio of the corrosion current densities $\gamma = i_{corr}/i'_{corr}$ is obtained [10–15]:

$$\gamma = \frac{i_{corr}}{i'_{corr}} = \frac{1}{1-\theta}e^{m\theta} \quad (3)$$

Pure geometric blocking action of the inhibitor may be described by the relationship $\gamma = 1/(1-\theta)$, or $\eta = 100\theta$, where η is the inhibitor efficiency expressed as a percentage of the corrosion rate decrease in the system containing the inhibitor with respect to the inhibitor-free system. It is worth stressing at this point that only in the case of pure geometric blocking of the electrode surface by the inhibitor can the efficiency, η, be treated as equivalent to the surface coverage θ [16].

On the other hand, with the stipulation that the blocking action term in Equation 3 can be neglected, exclusive influence on the kinetics of the dissolution reaction is expressed by the equation $\ln\gamma = m\theta$, where m is a constant.

Here, we present the analysis of corrosion inhibition properties of mimosa tannin on low-carbon steel in hydrochloric acid based on the results obtained from polarization and impedance spectroscopy measurements. The results are discussed, in particular, with respect to the inhibitor influence on partial anodic and cathodic reactions as well as with respect to the molecular properties of mimosa tannin obtained previously by the method of molecular modelling.

2. Experimental details

Polarization measurements were performed on cylindrical electrodes machined from low-carbon steel, sealed in epoxy resin, with a circular cross section exposed to the electrolyte. The electrolyte was 5% hydrochloric acid alone and with different inhibitor concentrations (10^{-5}–10^{-2} mol dm^{-3}), at a temperature of 40 ± 1 °C. The electrodes were cleaned by grit 600 emery paper, degreased in methanol, rinsed by doubly distilled water and immersed in test solutions for 3 h at the open circuit potential.

The polarization curves were recorded in the potential range ±200 mV E_{OCP}, at a scan rate of 1 mV s^{-1}. Impedance measurements were performed at the open circuit potential, E_{OCP} with a.c. voltage amplitude ±5 mV in the frequency range 10 mHz to 100 kHz.

Electrochemical measurements were performed using the SI 1287 Electrochemical Interface and SI 1255 Frequency Response Analyser. The reference electrode was a saturated calomel electrode and the counter electrode was a platinum foil.

Commercial mimosa tannin extract was used in this study. The structure of the mimosa tannin has been previously described by Seawell [17].

3. Results

Potentiodynamic polarization characteristics for low-carbon steel in 5% HCl containing various concentrations of mimosa tannin are shown in Figure 1. The open circuit potential E_{OCP}, the corrosion current density j_{corr}, the anodic and cathodic Tafel slopes, b_a and b_c, calculated by the Tafel extrapolation method are listed in Table 1.

The inhibitor addition decreases the anodic Tafel slopes and slightly increases the open circuit potential recorded after the three-hour-long electrode stabilization in solution.

A negligible change in the cathodic Tafel slopes indicates that hydrogen evolution is diminished exclusively by the surface blocking effect of the inhibitor. In this case, as proposed by Vračar and Dražić [18, 19], the surface coverage θ may be calculated using the following equation:

$$\theta(c_{inh}) = 1 - \frac{(i_{cat})_{c_{inh}}}{(i_{cat})_{c_{inh}=0}} \qquad (4)$$

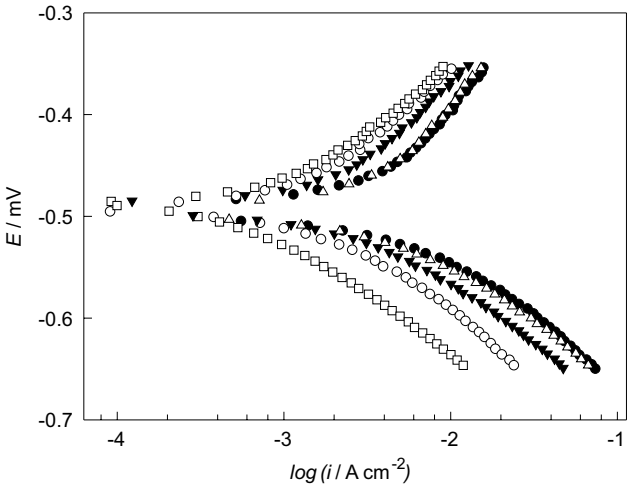

Fig. 1. Potentiodynamic polarization curves for low-carbon steel in 5% HCl at 40 ± 1 °C with various concentrations of mimosa tannin (● – 0, △ – 10^{-5}, ▲ – 10^{-4}, ○ – 10^{-3}, □ – 10^{-2} mol dm^{-3}).

where i_{cat} is the cathodic current density at constant potential, i.e. the rate of hydrogen evolution reaction (h.e.r). The values of θ calculated by applying Equation 4 at the potential of −0.6 V are also shown in Table 1.

The influence of inhibitor concentration on the impedance spectra of the investigated system is depicted in Figures 2 and 3. In all cases, the Nyquist plots in Figure 2, are not perfect semicircles, and in the Bode plots, in Figure 3, the slopes of the log Z against log f curves are not −1. Deviations of this kind are often referred to as the frequency dispersion of interfacial impedance. This anomalous phenomenon can be attributed to the inhomogeneity of the electrode surface arising from surface roughness or interfacial phenomena [20]. The equivalent circuit containing solution resistance, R_s, in series with the parallel network of charge transfer resistance, R_{ct}, and a constant phase element (CPE) substituted for the double layer capacitance, was used to model the experimental data. The corresponding transfer function of the total impedance, Z_{total}, for this circuit is given by

$$Z_{total} = R_s + \left[\frac{1}{R_{ct}} + Q\omega^n\left(\cos\frac{n\pi}{2} + \mathrm{I}\sin\frac{n\pi}{2}\right)\right]^{-1} \qquad (5)$$

where Q is the capacitance parameter, n is the parameter which characterizes the deviation of the system from ideal capacitive ($n = 1$) behaviour and I is the imaginary

Table 1. Potentiodynamic polarization parameters, inhibitor efficiency and surface coverage of low carbon steel by mimosa tannin in 5% HCl at 40 ± 1 °C at various inhibitor concentrations

c_{inh} /mol dm^{-3}	E_{ocp} /V	i_{corr} /μA cm^{-2}	b_a /V dec^{-1}	b_c /V dec^{-1}	η_{pol} %	θ
0	−0.501	3109.1	0.175	−0.110	–	–
10^{-5}	−0.500	2508.2	0.163	−0.102	19.3	0.11
10^{-4}	−0.496	1645.9	0.142	−0.108	47.1	0.41
10^{-3}	−0.493	1050.9	0.122	−0.110	66.2	0.65
10^{-2}	−0.484	612.9	0.116	−0.110	80.3	0.85

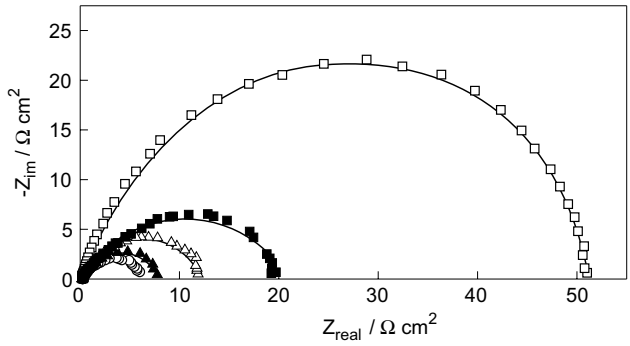

Fig. 2. Nyquist plots of impedance spectra of low-carbon steel in 5% HCl at 40 ± 1 °C with various concentrations of mimosa tannin (○ – 0, ▲ – 10^{-5}, △ – 10^{-4}, ■ – 10^{-3}, □ – 10^{-2} mol dm^{-3}).

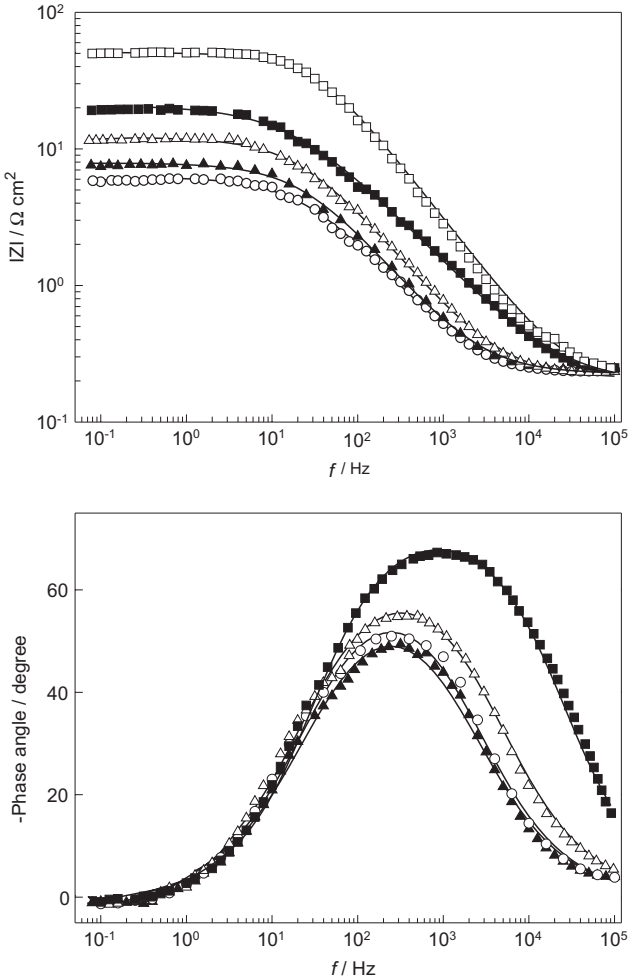

Fig. 3. Bode plots of impedance spectra of low-carbon steel in 5% HCl at 40 ± 1 °C with various concentrations of mimosa tannin (○ – 0, ▲ – 10^{-5}, △ – 10^{-4}, ■ – 10^{-3}, □ – 10^{-2} mol dm^{-3}). Solid lines represent the fits.

constant. When used instead of the double layer capacitance, CPE causes a rotation of the centre of the capacitive semicircle below the real axes by a frequency independent constant phase angle $\phi = (1-n)\pi/2$. For a perfect capacitor, $\phi = 0$ ($n = 1$), and for a perfect resistor, $\phi = \pi/2$ ($n = 0$).

Table 2. Impedance parameters and the corresponding inhibitor efficiency of mimosa tannin as an inhibitor of low carbon steel corrosion in 5% HCl at 40 ± 1 °C.

c_{inh} /mol dm^{-3}	R_s /Ω cm^2	$Q \times 10^6$ /Ω^{-1} s^n cm^{-2}	n	R_{ct} /Ω cm^2	η_{imp} %
0	0.222	3407.3	0.75	5.84	–
10^{-5}	0.226	2720.5	0.76	7.48	21.92
10^{-4}	0.195	1874.9	0.77	11.60	49.65
10^{-3}	0.211	1791.9	0.68	19.77	70.46
10^{-2}	0.202	242.7	0.82	50.61	88.46

The parameters R_s, Q, n and R_{ct}, determined for each set of experimental data, are shown in Table 2. An increase in the inhibitor concentration is accompanied by a decrease in Q and an increase in R_{ct}.

The inhibitor efficiencies, η, were calculated from the equation:

$$\eta(c_{inh}) = \frac{(v_{corr})_{c_{inh}=0} - (v_{corr})_{c_{inh}}}{(v_{corr})_{c_{inh}=0}} \quad (6)$$

where $(v_{corr})c_{inh}$ and $(v_{corr})c_{inh=0}$ are the rates with and without the presence of the inhibitor obtained from polarization measurements and impedance spectroscopy measurements. The corresponding inhibitor efficiencies were denoted as η_{pol} and η_{imp}, respectively, and are listed in Tables 1 and 2.

4. Discussion

The action of mimosa tannin as a corrosion inhibitor has been investigated previously in aqueous solutions of various pH [21–28]. In our previous investigations [28–30], it was found that mimosa tannin acts as an adsorption inhibitor in acidic solution. In particular, on the grounds of the energetic parameters deduced from the adsorption isotherms at pH $\leqslant$ 1, mimosa tannin was shown to be capable of forming a strong chemisorptive bond with the low-carbon steel electrode surface.

In order to establish the relationship between adsorption and corrosion inhibition, obtained from kinetic data, the logarithm of the coefficient γ is presented as a function of the surface coverage θ (Figure 4). The coefficient γ was calculated from polarization experiments by the equation $\gamma_{pol} = (i_{corr})_{c_{inh}=0}/(i_{corr})_{c_{inh}}$ and from impedance measurements by the equation $\gamma_{imp} = (1/R_{ct})_{c_{inh}=0}/(1/R_{ct})_{c_{inh}}$. Equation 3 was fitted to these data by the Levnberg–Marquardt nonlinear fit method implemented into the programming system *Mathematica*® and the resultant curve is shown in Figure 4. The value of m was found to be equal to −0.116 yielding the exponential factor in Equation 3 to vary between 1 for $\theta = 0$ and 0.89 for $\theta = 1$. This would mean that the energy effect expressed by the exponential term opposes the inhibitive effect introduced by the geometric blocking of the surface. According to Equa-

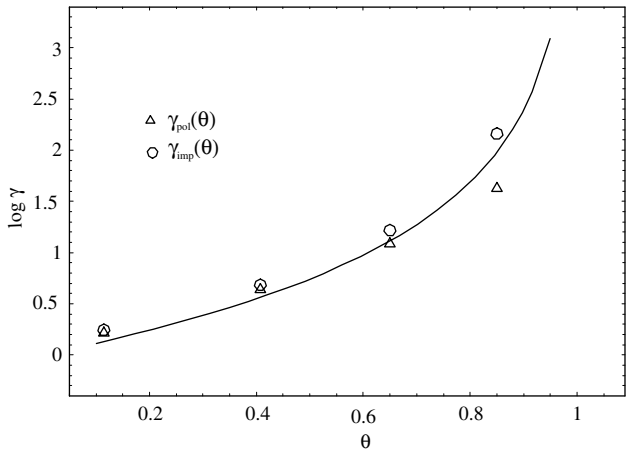

Fig. 4. Logarithm of the ratio of the corrosion current densities in the uninhibited and inhibited systems as a function of the surface coverage of low-carbon steel by mimosa tannin in 5% HCl at 40 ± 1 °C.

tion 1b, this kind of behaviour could originate from the lowering of the overpotential of the anodic reaction due to inhibitor adsorption and is in accordance with the observed decrease of b_a by inhibitor addition. In addition to the energy effect, the pronounced decrease in b_a could partly be due to electrochemical desorption of the inhibitor from the metal surface during dissolution [31].

The prevalance of the geometric blocking effect over the energy effect for the anodic reaction is, however, apparent from Figure 1, as the shift of anodic curves to lower current values is observed with the inhibitor addition.

The positive shift in E_{OCP} (Table 2) may be explained in terms of Equation 2. The term in square brackets calculated with the values of b_a and b_c from Table 1 is positive for the present system, therefore, the negativity of the parameter m and the corresponding negativity of $\Delta\psi_1$, indicate that a shift to positive values of E_{OCP} should be expected.

Concerning the adsorption and/or corrosion inhibition processes, the orientation of the adsorbed organic molecules at the metal surface is of special interest. It has been reported that the adsorption of heterocyclic compounds occurs with the aromatic rings sometimes parallel but mostly perpendicular with respect to the electrode surface [32, 33]. A similar system in which linoleic acid might be adsorbed at the mercury electrode in two different positions (parallel or perpendicular to the surface) was observed [34]. The method of scaling of a mercury electrode, used in this work, to obtain the fractal dimension of the adsorbed layer provides a sensitive means for the detection of phase changes in adsorption processes of linoleic acid, as dependent on fractional electrode coverage. In order to represent a system in which the organic substance is adsorbed at the electrode in two different positions, fractional coverage with flat (θ_1) and perpendicularly oriented (θ_2) molecules was given by:

$$\theta_1 = \theta(1-\theta) \quad \text{and} \quad \theta_2 = \theta^2 \tag{7}$$

where $\theta = \theta_1 + \theta_2$ is the fractional electrode surface coverage.

Consequently, the double layer capacitance should reflect the reorientation behaviour of the inhibitor very well if the molecules that adsorb are polar, with their dipole moment oriented preferably parallel or perpendicular to the longest molecule axes. The dipole moment of the four types of flavonoid molecules that comprise mimosa tannin, is almost perpendicular to the longest axis of the molecule [29]. The molecules with their longest axis oriented parallel to the surface would then have the dipole moment perpendicular to the surface and preferentially oriented in the direction of the electric field contributing to the microscopic value of the dielectric constant. The value of the tannin dipole moment varies between 1.91 and 2.81 D (depending on the type of the flavonoid molecule). It is comparable to the dipole moment of water of 1.85 D, indicating that the inhibitor influence on the double layer capacitance should be noticeable.

The double layer capacitance of the investigated system C_{dl}, has been calculated from the parameters Q an R_{ct} (Table 2), using the equation:

$$C_{dl} = \sqrt[n]{\frac{Q}{R_{ct}^{n-1}}} \tag{8}$$

C_{dl} is shown as a function of θ in Figure 5. The overall capacitance of the electrode | solution interface may be represented by three capacitors in a parallel connection:

$$C_{dl} = C_1(1-\theta) + C_2\theta(1-\theta) + C_3\theta^2 \tag{9}$$

where C_1, C_2 and C_3 denote the specific capacities of the electrode | solution interface in the supporting electrolyte (C_1) and the surface completely covered by the flat-lying molecules (C_2) and by the perpendicularly lying molecules (C_3), respectively. It is readily observed from Equation 9 that if there is no contribution from the adsorbed inhibitor layer to the interfacial capacity, the capacity decreases linearly with surface coverage as shown by the dashed line in Figure 5. By fitting Equation 9 to the experimental data in Figure 5, it was concluded that physically reasonable parameters ($C_1 = 875\ \mu F\ cm^{-2}$ and $C_2 = 226\ \mu F\ cm^{-2}$) could be obtained if only the first two terms of Equation 9 are taken into account. This means that the capacitance contribution from the inhibitor covered surface is solely due to the flat-adsorbed molecules at low surface coverage. The effect is relatively weak and indicates that the molecules probably change their position to a perpendicular one against the electrode surface, upon increase of the surface loading by the inhibitor. This finding corresponds to those obtained by the application of substitutional isotherms that has shown that on the average, one tannin molecule replaces four water molecules in the process of adsorption indicating the vertical orientation of the molecules on the surface, while the

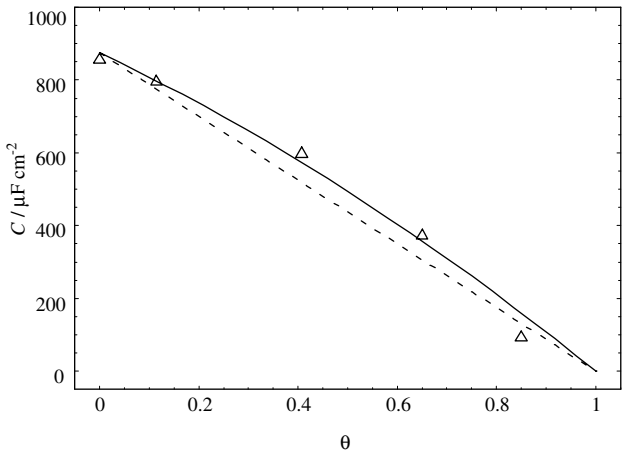

Fig. 5. The double layer capacitance as a function of the surface coverage. Solid line represents a fit. Dotted line represents the double layer capacitance dependency upon surface coverage under the assumption of no influence of the adsorbed inhibitor.

parallel orientation would yield a number of substituted water molecules between 7 and 10.

The prevailing parallel orientation of the dipole moment to the surface of the metal also explains why the energy effect exerted by the inhibitor, is relatively weak, since, according to the theory, only the dipole moments oriented vertically should alter the ψ_1 potential.

5. Conclusions

The treatment of corrosion inhibition data using adsorption isotherms and kinetic models is not an unambiguous procedure. Various measurable quantities deduced for the corrosion system with and without the inhibitor reflect the microscopic surface state of the system. Integral analyses of corrosion systems, as shown by the present study, would have to include both the adsorption and kinetic parameters analyses as well as system interfacial and inhibitory molecular properties, as indispensable means of elucidation of an inhibitor's protective action.

A theoretical model used in this work, based on the combined geometric surface blocking effect and the energy effect on partial anodic and cathodic reactions, enabled the correct interpretation of corrosion data characteristic of mimosa tannin action as an inhibitor of low-carbon steel corrosion in acidic solutions.

References

1. M. Metikoš-Huković and R. Babić, *J. Appl. Electrochem.* **26** (1996) 443.
2. Z. Grubač, R. Babić and M. Metikoš-Huković, *J. Appl. Electrochem.* **32** (2002) 431.
3. M. Metikoš-Huković, R. Babić and Z. Grubač, *J. Appl. Electrochem.* **32** (2002) 35.
4. M. Metikoš-Huković and R. Babić, *J. Appl. Electrochem.* **24** (1994) 325.
5. R. Babić, M. Metikoš-Huković, S. Omanović, Z. Grubač and S. Briniæ, *Br. Corros. J.* **30** (1995) 288.
6. M. Metikoš-Huković, R. Babić and A. Marinović, *J. Electrochem. Soc.* **145** (1998) 4045.
7. M. Metikoš-Huković, R. Babić and I. Paić, *J. Appl. Electrochem.* **30** (2000) 617.
8. M. Metikoš-Huković, K. Furić, R. Babić and A. Marinović, *Surf. Interface Anal.* **27** (1999) 1016.
9. B.B. Damskin, O.A. Petrii and V.V. Batarakov, 'Adsorption of Organic Compounds on Electrodes' (Plenum Press, New York/London, 1971) p. 305.
10. I.L. Rozenfeld, 'Corrosion Inhibitors' (McGraw Hill Inc., New York, 1981) p. 109.
11. V.N. Ponomarenko, Yu.V. Fedorov, Z.V. Panfilova, V.A. Sazonowa and V.N. Postnov, *Zach. Met.* **14** (1978) 595.
12. T. Szauer and A. Brandt, *Electrochim. Acta* **26** (1981) 1209.
13. T. Szauer and A. Brandt, *Electrochim. Acta* **26** (1981) 1219.
14. J. Lipkowski and Z. Galus, *Electroanal. Chem. Interfacial Electrochem.* **61** (1975) 11.
15. T. Biegler and H.A. Laitinen, *J. Electrochem. Soc.* **113** (1966) 852.
16. C. Cao, *Corros. Sci.* **38** (1996) 2073.
17. J. Seawell, *J. Oil Col. Chem. Assoc.* **61** (1978) 439.
18. Lj. Vračar and D.M. Dražić, *J. Electroanal. Chem.* **339** (1992) 269.
19. Lj. Vračar and D.M. Dražić, *Corros. Sci.* **44** (2002) 1669.
20. H. Shih and F. Mansfeld, *Corros. Sci.* **29** (1989) 1235.
21. D. Altura and K. Nobe, *Corrosion* **29** (1973) 433.
22. M. Schorr and J. Yahalom, *Corros. Sci.* **12** (1972) 867.
23. J. Flis and T. Zakroczymski, *J. Electrochem. Soc.* **143** (1996) 2458.
24. O.L. Lahodny-Šarc and F. Kapor, *Mater. Corros.* **53** (2002) 264.
25. J. Iwanov and Yu.I. Kuznetsov, *Zaschita Metallov* **26** (1990) 48.
26. J. Iwanov and Yu.I. Kuznetsov, *Zaschita Metallov* **27** (1991) 379.
27. S. Martinez and I. Štern, *J. Appl. Electrochem.* **31** (2001) 973.
28. S. Martinez and I. Štern, *Appl. Surf. Sci.* **199** (2002) 83.
29. S. Martinez, *Mat. Chem. Phys.* **77** (2002) 97.
30. S. Martinez and I. Štern, Proceedings of the 15th 'International Corrosion Congress', ICC (Granada, Spain, 2002) CD-ROM.
31. V.J. Dražić and D.M. Dražić, Proceedings of the 7th European Symposium on 'Corrosion Inhibitors', Vol. 5, Suppl. No. 9 (Ann. Univ. Ferrara, 1990) p. 99.
32. J.O'M. Bockris, A.K.N. Reddy and M. Gamboa-Aldeco, 'Modern Electrochemistry 2A', 2nd edn (Kluwer Academic/Plenum Publishers, New York, 2000) p. 969.
33. J.O'M Bockris and B. Young, *J. Electrochem. Soc.* **138** (1991) 2237.
34. D. Risovič, B. Gašparović and B. Čosović, *Langmuir* **17** (2001) 1088.
35. W. Plieth, *Electrochim. Acta* **37** (1992) 2115.